Solar observation

Rebecca Nguyen
(Dated: June 29, 2023)

In this report, we will be analyzing spectroscopic observations taken by the Swedish 1-m solar telescope. More precisely, performing spectra analysis by gaussian fitting the data to determine the central wavelength of all locations within the observation region. Thus, making it possible to create a doppler map. We discovered that the doppler map gives a better understanding of mass motion associated with granulation as a result of convection.

I. INTRODUCTION

Spectroscopic observations can be used to study the granulation pattern in the solar photosphere and estimate doppler velocities of mass motions due to convection. In order to do so, we will by analyzing spectral data taken by the Swedish 1-m Solar Telescope (SST) on La Palma, more specifically data from the instrument CRISP. The data has dimensions (y, x, λ_i) = (550, 750, 8) with spatial units px and λ_i corresponds to 8 wavelength locations with index $i \in [0, 7]$.. For spatial dimension (y_i, x_i) we extract all wavelength locations within and obtain the spectral line. Considering spectral lines closely resemble a gaussian function it is appropriate to fit a gaussian to these data. We can estimate central wavelengths for all spatial dimensions from a gaussian fitted curve. Which will be used to estimate the doppler velocities of our field of view, relative to the spectra averaged over the whole region. By having doppler velocities of all spatial dimensions we can create a doppler map that describes the granulation pattern caused by convection.

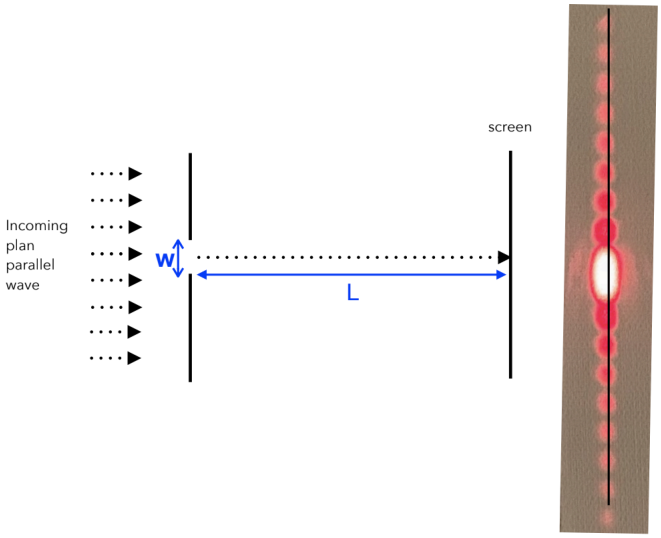

Figure 1. Single slit diffraction. [1]

The bright spots are where the waves constructively interfere with each other and the dark areas are where they destructively interfere. In order to obtain a more defined interference pattern with higher intensity, we create more slits. Diffraction with many slits is called a diffraction grating. The number of slits in diffraction grating is measured in lines per cm and there could be up to 1000's lines per cm [2]. Diffraction gratings are used to spatially separate light of different wavelengths. In terms of spectral analysis, diffraction grating has replaced prisms in most fields.

II. THEORY

A. Slit-spectrograph

Single-slit diffraction is a phenomenon in which waves are passed through a narrow slit. This cause a interference pattern of light and dark bands projected onto the screen, see figure 1.

B. Fabry-Perót interferometer

Fabry-Perót interferometer (or étalon) is an optical instrument widely used for spectroscopy, among many other purposes. In our case, we are interested in how Fabry-Pérot interferometer is used to measure the wavelengths of light.

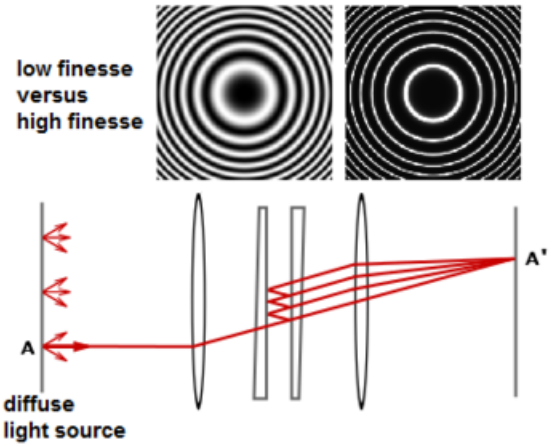

Figure 2. The set up of a Fabry-Pérot interferometer. [3]

The setup shown in fig 2 consists of two highly reflective surfaces (ex. mirrors) separated by a distance d. This creates an optical cavity in which the incident wave is bounced between the mirrors resulting in transmission and reflection. The purpose of the mirrors is to create a path length difference between subsequent transmitted waves. Only a small fraction of the waves are transmitted and the majority are reflected. This allows for plenty of subsequent reflections and transmissions between the two mirrors. The result is many waves interfering with each other and focused with a lens onto a screen/ detector. From this, we obtain an image produced by light and dark circles known as an airy disk. Complete constructive interference results in brighter circles and partially constructive interference results in darker circles. Fabry-Pérot interferometer can be used to determine wavelengths with a known distance d and incident angles θ, and vice versa [4].

C. Difference/similarities in slit-spectrograph and Fabry-Perót interferometer

These two ways of obtaining spectral observations are similar in the sense of using interference patterns of light to observe certain wavelengths of light. What differentiates Fabry-Pérot interferometer from slit spectrographs is Fabry-Pérot interferometer allows for tunable filters. This is beneficial by providing freedom in which spectral line we want to observe. However, slit spectroscopy does not allow for such freedom in choosing wavelengths of interest. Fabry-Perót interferometer also produces high-resolution interference patterns as the light bounces between the mirrors multiple times. In order to produce such a high-resolution pattern with a slit-spectrograph, we require more slits. Consequently causing complications in the sense of having different gratings for different purposes and having to consider this when performing an experiment. Rather than mostly just changing the distance between two mirrors in PFI.

D. Examples of instruments and telescopes

Examples of telescopes performing solar observations are the Swedish 1-meter Solar Telescope (SST) on La Palma and Interface Region Imaging Spectrograph (IRIS) which is a NASA solar observation satellite.
SST uses two instruments named CRISP and CHROMIS. They both use Fabry-Pérot interferometers and observe different wavelengths. CHROMIS observes in wavelengths 3000-4000Å, while CRISP observes in 6000 - 8000Å [5].

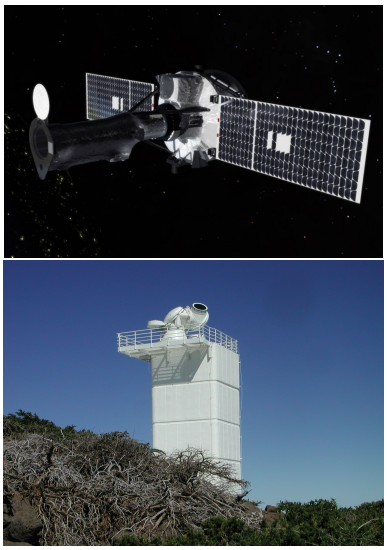

Figure 3. IRIS [6] depicted in the image on top and SST [7] on the bottom.

SST is the largest European solar telescope and number one worldwide in terms of high spatial resolution. This telescope allows the study of the solar structure in unprecedented detail [8]. For example, this telescope observes solar granulation patterns in high resolution.

E. Granulation pattern

The granulation pattern on the solar photosphere appears to be due to convection in the layer below (convective zone). The light yellow spots in figure 4 are called granules or granulation cells. Hot matter rises from the center of the granules and the energy is radiated away on the surface. The cooler matter flows back down through the intergranular lanes which are the dark lines around the granules. The lanes appear dark because the matter has been cooled down. The granulation pattern is not static and continuously evolves due to convection. [9]

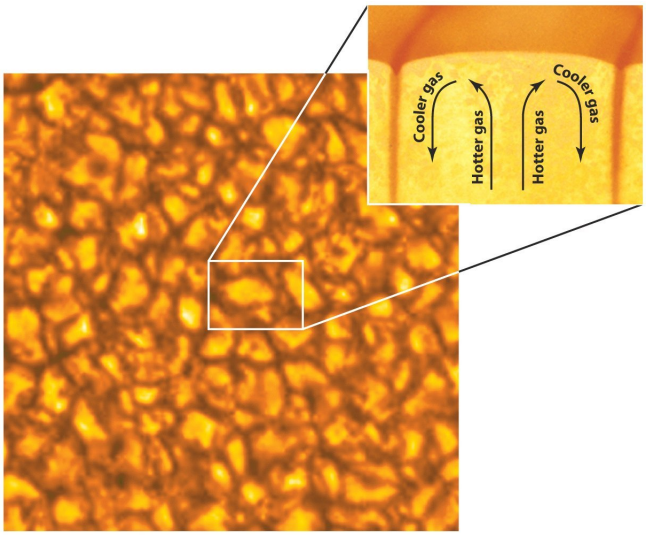

Figure 4. Illustration of convection within the granules in the granulation pattern on the solar photosphere [10].

F. Doppler effect and velocity

From the granulation pattern of the solar photosphere, we obtain absorption spectra. This data can be used to find the doppler velocities. The purpose is to find the mass velocity associated with granulation as a result of convection.

Doppler effect describes how waves are perceived when moving away or towards an observer (the same effect can be applied to a moving observer with the same basic principle). Meaning it is a relative measurement and will only make sense when measured relative to something. For a more intuitive understanding, one can think of an ambulance passing by as our reference.

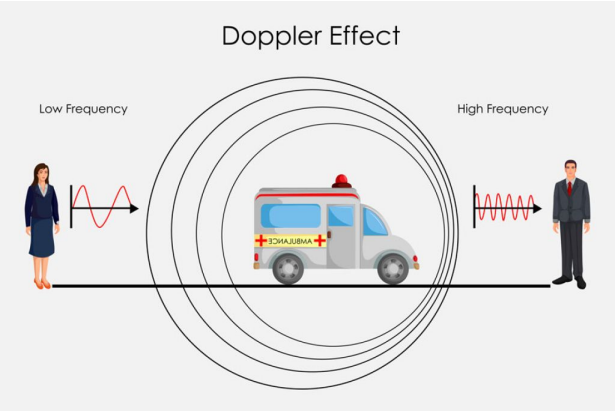

Figure 5. Illustration of how waves are affected by the Doppler effect [11].

As the ambulance is moving toward an observer the sound waves are compressed, causing the frequency to increase and the wavelength to shorten. See fig II F. As the car is moving away from an observer, the opposite happens and the sound "elongates".

The Doppler effect not only applies to sound but also to light. For a light source moving towards the observer, the observed wavelength is shorter than the emitted wavelength $\lambda + \Delta\lambda$, making it blueshifted. For the opposite case when the light source is moving away from the observer, the observed wavelength appears longer $\lambda - \Delta\lambda$, making it redshifted.

The Doppler velocity can be calculated by equation 1

$$v = \frac{\lambda_{observed} - \lambda_{emitted}}{\lambda_{emitted}} \cdot c = \frac{\Delta\lambda}{\lambda} \cdot c \tag{1}$$

The wavelength window in our dataset is centered around Fe I, 6173 Ångstrom [Å], which is a spectral absorption line that maps the photosphere [13]. The doppler velocity of different areas in the granulation pattern can be calculated by using the spectra of the given area and equation 1. Where c is the speed of light, $\lambda_{emitted} = 6173\mathring{A}$ and $\lambda_{observed}$ is given in the spectra.

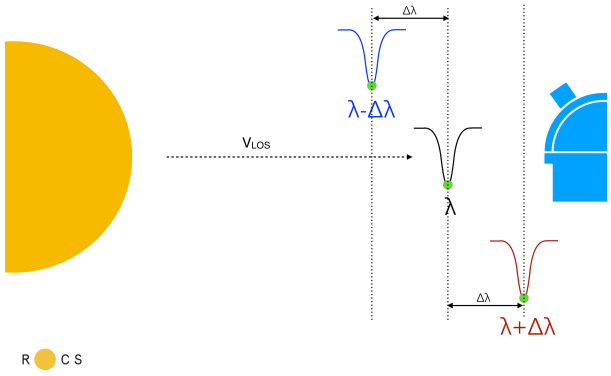

Figure 6. Observed wavelength from the sun at different locations. [12].

Measuring the Doppler shift (of light) from individual granules provides evidence of mass velocity motions as a result of convection. The reason for this is when hot matter rises to the surface, we observe a blueshift as the light source moves toward us. Vice versa for the cool matter which flows back and causes observed redshift.

III. METHOD

The spectroscopic observations were obtained from a Fabry-Pérot interferometer within the instrument CRISP. The observation data are from a rectangular region on the sun. The spatial dimension of this data is (y, x) = (550, 750) with spatial resolution 0.058 arcsec per pixel (1 arcsec = 740 km on the photosphere) [13]. This corresponds to a physical size of 759 877 140 km^2 on the photosphere.

The data was stored in two data files: `idata_square.npy` and `spect_pos.npy`. The file `idata_square.npy` has dimensions $(y, x, \lambda_i) = (550, 750, 8)$, containing spectral data (intensity observed as a function of wavelength, λ). The spatial units are given in px and λ_i corresponds to the 8 wavelength locations. `spect_pos.npy` contains the wavelength value given in Ångstrom for the 8 wavelength locations in `idata_square.npy` per location (x, y).

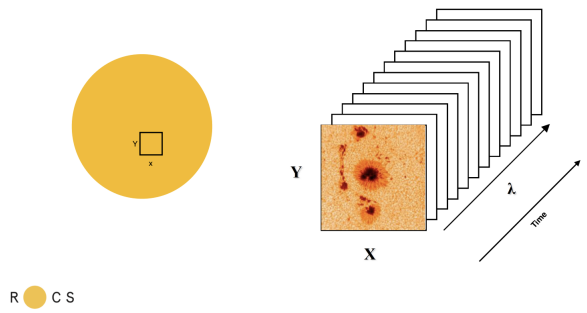

Figure 7. Illustration of how the `idata_square.npy` file looks like within our rectangular region (x, y) on the sun [12].

For each location/pixel (x_i, y_i) in the field of view we were able to plot the spectral line, more specifically absorption lines. The data of absorption lines closely resemble a gaussian curve and it is, therefore, an interest to curve fit a gaussian to these data. The equation for a gaussian is given in eq 2 below.

$$g(x, \mathbf{P}) = ae^{-\frac{(x-b)^2}{2c^2}} + d; \ \mathbf{P} = (a, b, c, d) \qquad (2)$$

Gaussian fitting is all about optimizing parameters in P based on the data for the spectra. The different parameters are as follows

a: the amplitude of the gaussian which should be negative for absorption lines. The difference in the minimum value of your spectral line and the minimum.
b: the mean of the gaussian. The position of the peak on the x-axis.
c: the standard deviation.
d. y-value of the baseline. The maximum value of your spectral line [13].

In python, we made use of `scipy.optimize_curve` fit as our gaussian fitting routine with eq. 2, x = `spect_pos.npy`, y = wavelength spectra for a given coordinate and estimated parameters (a, b, c, d) as arguments. By doing so we got a new set of optimized parameters (a, b, c, d) for the gaussian fitted curve which suits our datapoints the best. The purpose of doing a gaussian fit is to easier extract the peak value, b, in order to determine the wavelength of any given absorption line. From the value b, we can calculate the doppler velocity for the location using eq.1, and create a doppler map to better understand the granulation pattern on the solar photosphere.
We will also be gaussian fitting the average spectra of the whole field of view in order to determine the spectral absorption line that maps the photosphere, meaning the wavelength emitted from the sun. This can be done by measuring the mean value of all spectra data in `idata_square.npy` and gaussian fitting that data. This is an interest due to doppler velocities being a relative measurement, and in our case, the wavelength emitted from the photosphere.

IV. RESULTS

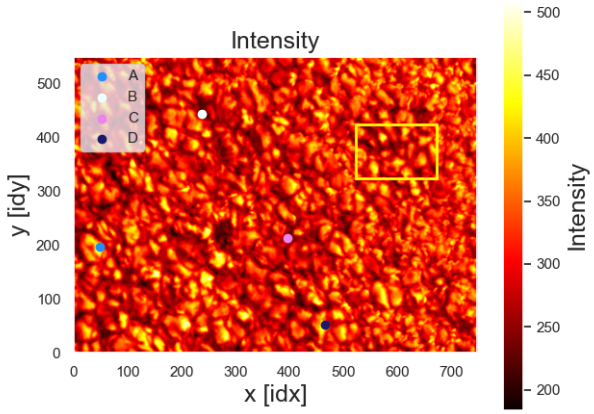

Figure 8. Intensity observed as a function of wavelength for a rectangular region on the sun (field of view).

The figure above displays the intensity data from `idata_square.npy` for one wavelength on the entire grid. In this case it is shown for wavelength index $\lambda_i = 4$, see fig. 7 for better understanding.

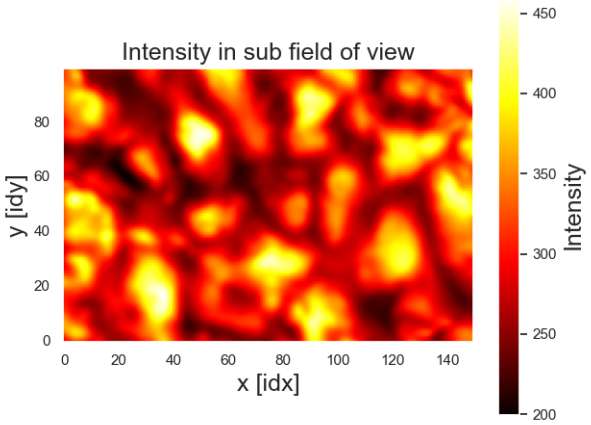

Figure 9. Sub field of view of intensity plot in fig 8

The plot of the data within the yellow rectangle in fig. 8, also named the sub field of view.

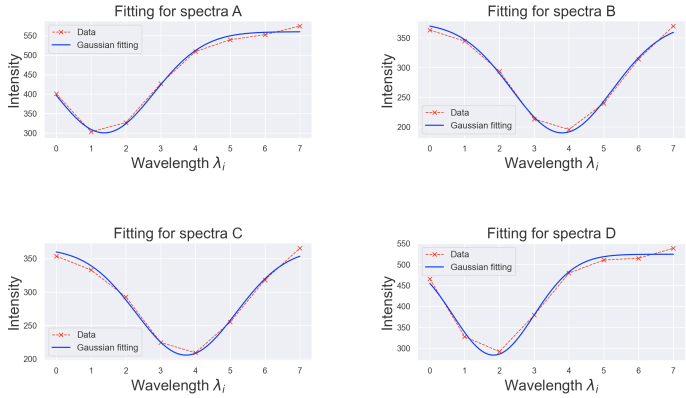

Figure 11. Gaussian fitting of spectra for points A - D

A plot showing the gaussian fitting for all 4 observation points. "Data" refers to the spectra retrieved from `idata_square.npy`.

As fig. 10 and fig. 11 are difficult to read, I have added scaled up versions in appendix A.

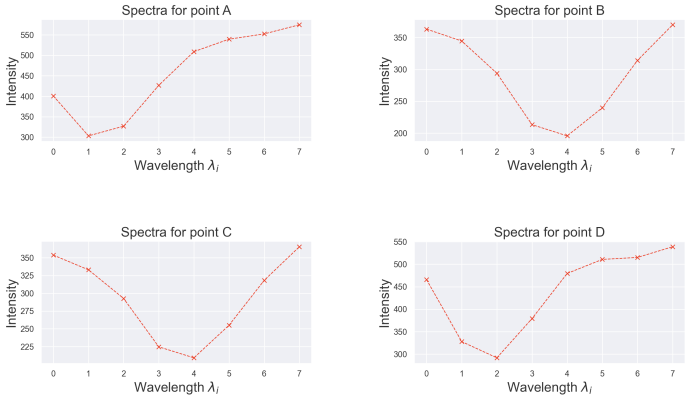

Figure 10. Spectra for observed intensity at points A, B, C and D.

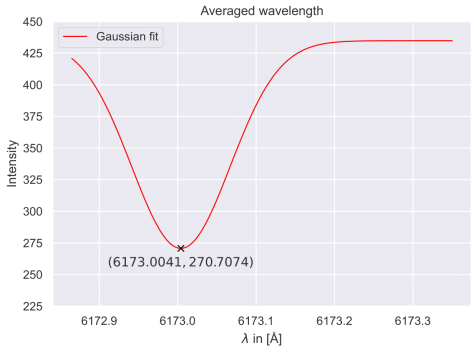

Figure 12. Estimated central wavelength of the Fe I absorption line.

Spectra lines for 4 observation points: A at (x, y) = (49, 197) px, B at (x, y) = (238, 443) px, C at (x, y) = (397, 213) and D at (x, y) = (466, 52) px. Locations of points are marked in fig 8.

The spectra averaged over the whole region, this time plotted with the wavelength values [Å], retrieved from `spect_pos.npy`, instead of index numbers like in fig. 10 and fig. 11. The central wavelength (peak) of the FE I absorption line is marked with an 'x' in the figure.

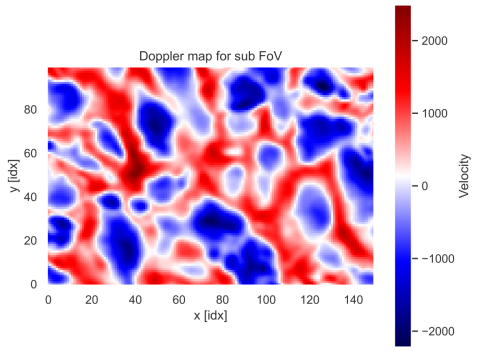

Figure 13. Doppler map of the sub field of view

A plot of doppler velocity relative to the averaged wavelength, at every pixel within the sub field of view.

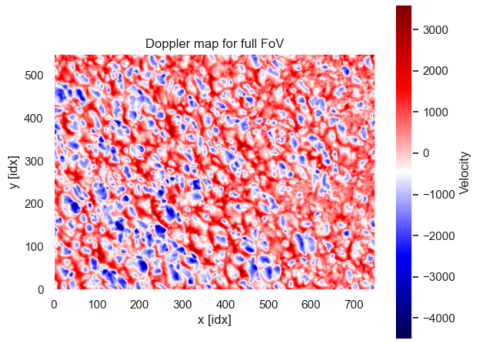

Figure 14. Doppler map of the field of view

Table I. Doppler velocity of points A, B, C, and D

Observation point	Doppler velocity
A	-3744.566 m/s
B	1606.148 m/s
C	1439.322 m/s
D	-2752.272 m/s

Doppler velocities of our 4 observation points within the field of view.

V. DISCUSSION

A. Average spectra

In figure 12 we have estimated the central wavelength of the Fe I absorption line by gaussian fitting the mean of spectra data in `idata_square.npy`. The peak in the gaussian fitted curve is placed at 6173.0041 Å which is the wavelength window of spectral absorption line that maps the photosphere, as mention in subsection II F.

B. Intensity image

The intensity image of field of view can be found in fig. 8 and of sub field of view can be found in fig. 9. These figures show what data obtained from `idata_square.npy` looks like. Now in order to discuss the granulation pattern, I choose to interpret the sub field of view as the figure is zoomed in and easier to study. The granulation pattern we are looking at is due to convection. In the figure, we observe multiple cells which have a yellow center and red/black outline. These are called granules. The center of the cells is yellow because they have higher intensities caused by hot matter rising from the center of the granule. The darker parts indicate the path in which the cooled matter travels back down to the convection layer underneath the photosphere. Zooming back out to the full field of view we are able to see where our observation points are placed. Points A and D are placed almost in the center of two granules, meanwhile, points C and B are placed on a darker part. From this, we understand that for points A and D we are observing hot matter rising to the photosphere and vice versa for points B and C.

C. Spectra and gaussian fitting

The spectra for observation points A-D can be found in fig. 10 for the raw data and fig. 11 for the gaussian fit. Based on the granulation pattern given in fig. 8, I expect spectra of A and D to be blueshifted and their peaks to be placed further left (on values of shorter wavelengths) than the average spectra line. The reason for my expectations is the fact that points A and D are placed almost in the center of the granules. The central part of a granule is where matter rises to the surface and from our point of view, it looks like the matter is moving toward us. From the doppler effect, this results in a blueshift i.e. shorter observed wavelength. For points B and C, I expect a redshift, the peak of the spectra line placed further to the right than the average spectra and therefore longer observed wavelength based on the same principle as for points A and D (but opposite effect).

D. Doppler velocities

The doppler velocities of points A - D are given in table I. From eq. for doppler velocities 1: $\lambda_{observed} < \lambda_{emitted} \rightarrow v < 0$). As discussed in previous subsections, point A and D are blueshifted which results in longer observed wavelengths, and the opposite for point B and C. From this, we expect negative values for A and D, but positive values for B and C.

E. Doppler map

From the gaussian fitting of the spectra lines, we were able to create doppler maps for both field of view and sub-field of view. Due to the same reasoning as the intensity image, I choose to only interpret the doppler map for sub field of view, 13. In the figure, we are able to observe the granulation pattern in terms of doppler velocity. The blue shapes are the central parts of granules where the hot matter arises. They are blue-shifted due to rising matter being equivalent to light moving toward us, the observers. We observe a shorter wavelength from the rising matter as it rises to the solar photosphere. As it cools down it moves back down to the layer beneath the solar photosphere, which results in a redshift. We check this by comparing it to the intensity image of sub field of view. We notice a similarity in the shape of solar granules. This can be interpreted as high intensities being related to the blueshift and lower intensities related to the redshift. Though, this makes me wonder how intensity is related to temperature. The parts of the granulation pattern with high intensities are locations where the hot matter arises. This can be explained by approximating the sun as a black body (although not always a good approximation). For a black body, as temperature increases, the intensity of all wavelengths increases. The same principle applies to the opposite effect.

The doppler map, however, has a rather clean distinction in where the hot matter arises and where the cool matter returns. They are either seen as blue or red, making it easier to "read" the granulation pattern compared to the intensity plot.

VI. CONCLUSION

The purpose of our investigation was to analyze doppler velocities of the granulation pattern in the solar photosphere.

Data was received from SST and contained spectral data. We studied the spectra of each pixel within our data, which covered a region of (550, 750) px or 759 877 140 km^2 on the solar photosphere. The spectral data were fitted with gaussian curves in order to estimate the central wavelength of each location. We had 4 observation points in which we visualized the spectra lines and their gaussian fit. These are the spectra lines shown under section IV.

Central wavelengths obtained were then used to estimate the doppler velocities of our field of view and to create a doppler map for both the full field of view and the sub-field of view.

From our results, we noticed the plots of intensity and doppler velocities looked similar. We discovered that the central area of granules in which hot matter rises to the solar photosphere results in a blueshift from our point of view. We observe shorter wavelengths as it looks like the matter is moving toward us. While matter cools down and returns back to the convective zone through intergranular lanes we observe shorter wavelengths, thus resulting in redshift. This was measured relative to the wavelength window centered around 6173 Å which maps the photosphere.

For future studies, it might be better to include the error margin of our analysis. This would give a better understanding of how good our data actually is. In addition to giving a reference of what can be improved in our analysis. It would also be beneficial to know about signal to noise ratio of data, but I believe in our case it was beyond the scope of our investigation.

ACKNOWLEDGMENTS

I would like to thank the physics association for bachelor students at UiO for providing coffee and a place for discussion (though, mostly collective confusion).

Appendix A: Spectra lines and their gaussian fitted curve

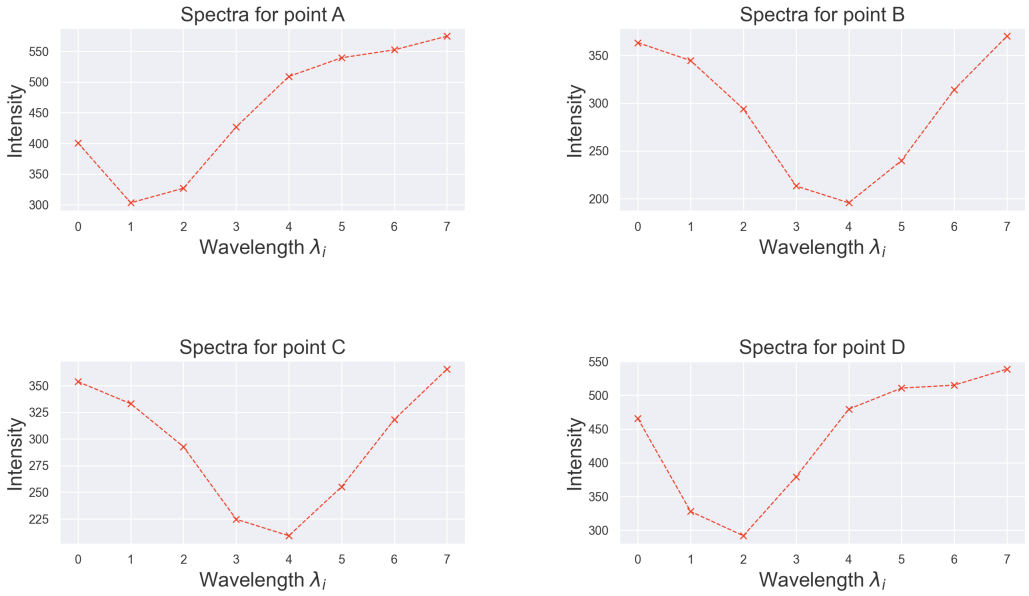

Figure 15. Spectra for observed intensity at points A, B, C, and D, scaled up version of fig. 10

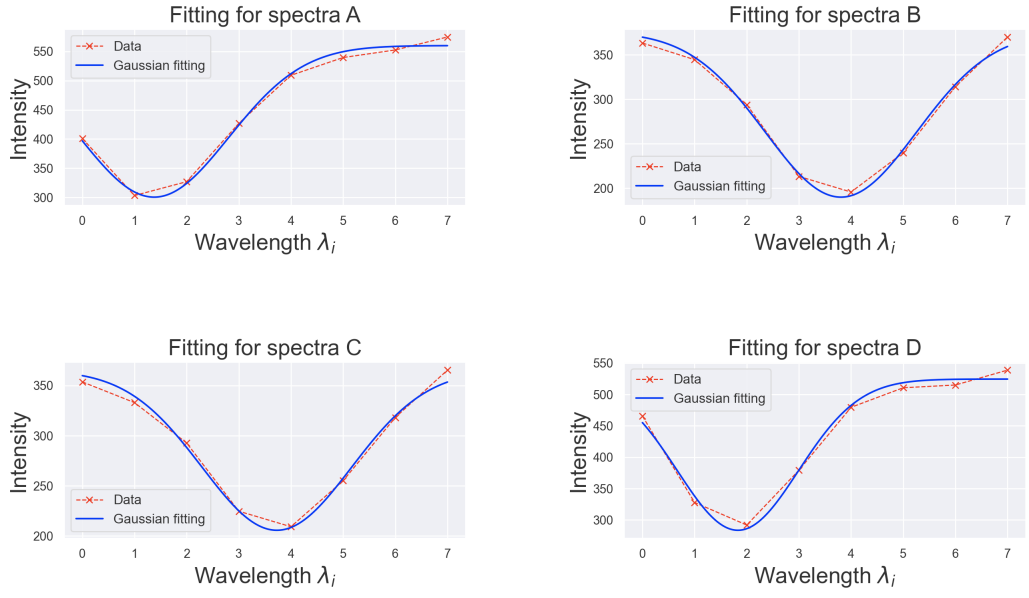

Figure 16. Gaussian fitting of spectra for points A - D, scaled up version of fig. 11

Appendix B: References

[1] Nancy Narang, 2022. Solar day 1 presentation
[2] Diffraction grating — Light waves — Physics — Khan Academy
[3] Fabry-Pérot interferometer image
[4] Fabry Perot Interferometer video
[5] CHROMIS and CRISP images
[6] Image of Iris
[7] Image of SST
[8] Instituto de Astrofísica de Canarias. Swedish Solar Telescope
[9] Wikipeda. 2022. *Solar granule*. Fetched: 02.10.2022. Solar granule
[10] Solar granulation image
[11] Doppler effect image
[12] Nancy Narang, 2022. Solar day 2 presentation
[13] Claudia Cicone, 2022. Assignment 1 description